Using Thermal Shape Memory Alloys to Actuate Origami-Inspired Compliant Mechanism

T.K. van der Graaf (4591399), J.T. Klappe (4571940), M.N. Ligthart (4561813) & S.Ö. Rietmeijer (4591267)
BEP-GROUP PME-A6 OF DELFT UNIVERSITY OF TECHNOLOGY

***Abstract*— In order to achieve insights in actuators for origami-inspired compliant mechanisms, an exploratory research has been conducted to different actuation strategies. Thermal shape memory alloys have the highest potential to meet the requirements of this research and experiments have been executed to investigate the behaviour of the material. The results of the experiments, where the blocking moment of the test sample has been measured, have been compared to values by Brinsons formula. From these results it can be concluded that thermal shape memory alloys do have the potential to be used as actuator in origami-inspired compliant mechanisms, yet further research is needed to realize this concept. It is recommended to focus this follow-up research on the programming technique of the material, the origami structure in which the material should be implemented, and the crystalline arrangement and martensite fraction within the material.**

I. INTRODUCTION

The capability of micrometre scale devices is limited by existing manufacturing methods. This limitation can be conquered by using origami-based methods. 3D compliant mechanisms can be made out of planar materials [8]. However, one of the main problems is the integration of a reliable actuation method into the origami mechanism. Another problem is the miniaturization challenge that occurs. This research is aimed to achieve better insights in (the design of) one-layer actuation integrated within an origami structure. To actuate the origami structure of this study, it is required to apply a moment on the structure. Previous research showed possible working principles for integrated actuators in compliant mechanisms, such as chemical, thermal, magnetic, and electrical actuation principles [3]. Within this exploratory research, these different actuation strategies have been studied to design a fitting actuation system. It is preferred to have a working principle where no transmission is required, due to the friction losses which occur on microscale when a transmission is included. Thermal shape memory alloys (SMAs) had the greatest potential out of the selection of actuation principles and do not need a transmission due to the simplicity of the possible configurations. Within this paper the authors will go over the theory behind thermal shape memory alloys, followed by the methodology and results of the experiments, and will draw a conclusion regarding the research goal. Some recommendations will be made for further research on this topic.

II. THEORY

After a broad literature study on different working principles, the main focus was on thermal actuators, in particular thermal shape memory alloys [3]. This choice was based on the potential of the different principles to reach the requirements of this research. These requirements were set to make a feasible actuator for an origami inspired compliant mechanism. The set of requirements consisted of the following statements: the actuator must (1) make a deflection of 30°, (2) repeat the same movement five times with a maximum deviation of 5°, (3) work on macroscale, and (4) be scalable to microscale. Here, the need of a transmission to reach the required deflection was poorly judged due to the undesired friction losses this would add to the system.

In the next section, the material science of thermal SMAs shall be elaborated. Here, the focus will be on the shape memory properties of the material. The other property of thermal SMAs is its super elasticity. In this configuration the transition temperature of the wire is below its operation temperature. This causes the wire to always return to the programmed shape, which gives the material its super elastic property [6].

A. Thermal Shape Memory Alloys

The SMA has a transition temperature above its operation temperature. This means the material has shape memory properties [9]. Using thermal energy, the crystalline arrangement of the material can be modified. This causes the wire to shape towards a certain programmed configuration, when heated up to the transition temperature.

The material crystalline arrangement of the thermal SMA is either twinned martensite, detwinned martensite or austenite [1]. To program the shape memory wire into a shape, it should be annealed into the desired shape at 500°C (annealing temperature)[12]. Once the shape memory wire cools down, it returns to a twinned martensitic crystalline structure [1]. When the shape memory wire is deformed, the crystalline arrangement will transform from twinned martensite to detwinned martensite (this process is called twinning) [1]. Whenever the shape memory wire is heated up to its transition temperature, which is lower than the annealing temperature, the crystalline arrangement will return back to the austenite arrangement. This implies that the wire will go back to its original programmed shape [1]. The transition temperature depends on the composition of the shape memory alloy and is generally lower than 100°C [11]. This process is further elaborated in figure 1 where it is applied to a shape memory spring.

Some exceptional benefits of an thermal SMA as actuator are (1) the absence of transmission, (2) the low driving power (which is lower than equivalent working principles), (3) there exists suitable fabrication processes when NiTiCu is used as a micro-actuator, and (4) the response speed, which is relative slow at macro-scale, is alleviated drastically when the system is miniaturized [5].

The force that is generated through changing from detwinned martensite to austenite can be described with a

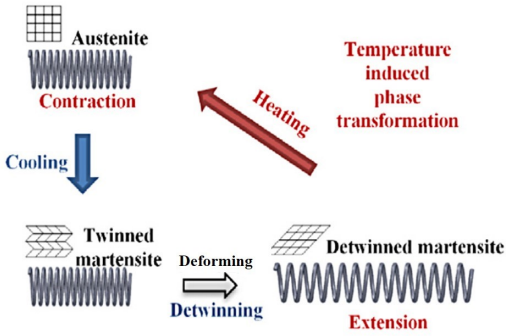

Fig. 1. Material Crystalline structure of SMA

phenomenological model that can be used when a shape memory wire is analysed out of engineering point of view [2], [10]. The equation for this model is shown in equation 1.

$$\sigma - \sigma_0 = E(\epsilon - \epsilon_0) + \Omega(\zeta - \zeta_0) \tag{1}$$

Where σ is the stress, E is the Young's modulus, ϵ is the strain, ζ is the martensite fraction and Ω is the stress tensor which is equal to $\Omega = -E\epsilon^t_{max}$. The initial stress and strain is equal to zero so $\sigma_0 = 0, \epsilon_0 = 0$. When using following relations: $\sigma = \frac{My}{I} = \frac{F_{sma} d_{sma} y}{I}$ $y = \frac{d_{sma}}{2}$. and $\epsilon_{sma} = \frac{\theta d_{sma}}{L_{sma}}$, equation 1 can be rewritten as equation 2. This indicates that the relation between the moment M and angle θ is linear.

$$M = \frac{2EI}{d_{sma}}\left(\frac{\theta d_{sma}}{L_{sma}} - \epsilon^t_{max}(\zeta - \zeta_0)\right) \tag{2}$$

In order to simulate the moment from this equation, both martensite fractions (ζ and ζ_0) need to be known. Within this study, the martensite fraction while the system generates the moment is unknown. Therefore, equation 2 will be simplified to equation 3.

$$M = \frac{2EI}{L_{sma}}\theta \tag{3}$$

In the design (which is described in section III) the thermal SMA wire has to generate a moment which is large enough to overcome the stiffness of the wire that is not actuated. The SMA wire which is not actuated operates as a hinge. The stiffness can be described by equation 4 that approximates the stiffness as a torsion spring connected to a free end beam [4]. This an approach that holds for deflections of a flexible beam.

$$K_1 = \pi(\gamma)^2 \frac{EI}{l} \tag{4}$$

Where K is the stiffness in Nm/rad, γ is a dimensionless constant equal to 0.85, E the Young's modulus, I the moment of inertia and l the length of the hinge.

Because the hinge is not an open end-body but a connection between two bodies, the hinge will be approximated in equation 5 as a beam connected to a torsion spring on each side. The moment needed to overcome the stiffness of the hinge depends on the bending angle. The wire that is not actuated is programmed at 90°. Therefore, at a bending angle of 90°, there is no moment needed to overcome the stiffness of the hinge. At other angles, the stiffness is modelled as a linear line with slope K. The moment needed to overcome the stiffness of the hinge and the generated moment of the SMA wires, equation 6 and equation 3 respectively, are plotted in figure 2. The two lines intersect at an angle of 48.6° . This is the expected equilibrium that will be reached when the test sample will be actuated from the bent to the flat position.

$$K = \pi(\gamma)^2 \frac{EI}{l} + \pi(1-\gamma)^2 \frac{EI}{l} \tag{5}$$

$$M = -K(\theta - \theta_{programmed}) \tag{6}$$

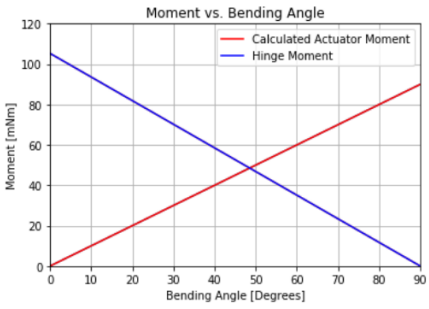

Fig. 2. Calculated Moment and Stiffness of Hinge vs. Bending Angle

III. Methods

As mentioned in section I, the actuation will be integrated into an origami-inspired compliant mechanism. The origami structure will act like a gripper when a moment is applied to the middle links, see figures 3 and 4 for further clarification of this movement. Considering only the middle links will be actuated, the test piece solely consisted of this part of the origami structure. These links were 3D printed two times; taped to both sides on a piece of paper; had a groove wherein the SMA wire would fit and this wire was ensured into its place by tape, see figure 5.

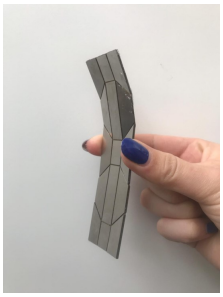

Fig. 3. Origami-Inspired Compliant Mechanism Rested

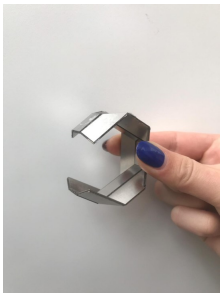

Fig. 4. Origami-Inspired Compliant Mechanism Actuated

Experiments during this research were executed using a 0.5 mm diameter thermal SMA wire (in particular NiTiCu, which consists of 47wt% nickel, 45-47wt% Titanium, and 6-8wt% Copper). The transition temperature of this SMA is

between 55 and 60°C. Using Joule heating, the wire was heated to approximately 70°C by running a 1.5 A current through the wire for 15 seconds [7]. To program the wire into the desired shape, it was formed using an aluminum mould and then, by way of using a blow torch, the wire reached a glowing state after which the blow torch was turned off. This state had reached the annealing temperature of 500°C.

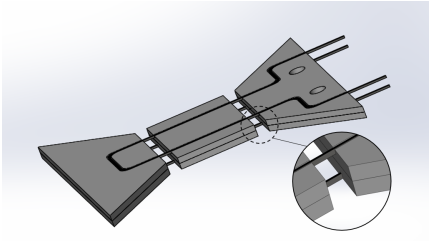

Fig. 5. Test Sample with Enlargement of the Hinge

The experiments were executed to measure the blocking force of the material at 30°, 60°, and 90° of β, for further illustration of this setup see figure 6. To fit the test piece into the test setup, two holes were integrated into the design so it could be placed above a 100 gram load cell. The test piece was manually put into angle β, the load cell was placed perpendicular to it, and the blocking force was measured when the SMA would move towards its programmed straight position using LabVIEW. An important note here is that the force measured is double the force a single wire could deliver due to the loop of the SMA in the test piece. This process was filmed and the footage was processed using ImageJ, thus the error in measuring β was estimated on 1° and the error of length d was estimated on 1 mm. During this experiment, three different test pieces were used and every piece was measured for each β five times.

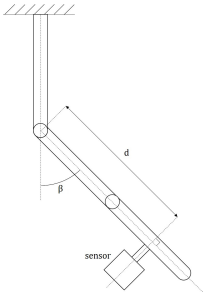

Fig. 6. Test Setup Blocking Moment

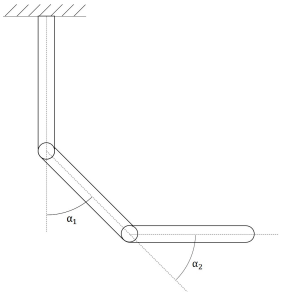

Fig. 7. Test Setup Repeatability

The configuration shown in figure 7 is used to measure the ability of the SMA to repeat the same actuation towards the straight and bent configuration five times. Three test pieces were used. For each test piece, two SMA wires were used, where one is configured to the straight position and the other to a configuration where both α_1 and α_2 are 90°. The wires are actuated by turns of ten seconds through the power supply, with a cooling period of 20 seconds in between each turn. These experiments were also filmed and the footage was processed using ImageJ to measure α_1 and α_2. In section IV the mean and the standard deviation are presented of these measurements using the difference between the straight and bent angle, $\Delta\alpha_1$ and $\Delta\alpha_2$.

IV. Results

A. Blocking Moment Experiments

In figure 8 the blocking force multiplied with length d (hence, the blocking moment) is plotted against the angle in which the test piece was bent. Each test piece is indicated with a different colour. The standard deviation of each piece is specified to indicate the error of the blocking moment. The standard deviation for the angle is neglected because it is mainly dominated by measuring errors.

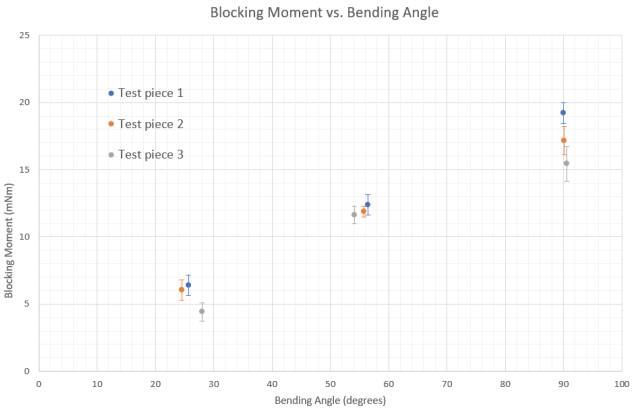

Fig. 8. Blocking Moment vs. Bending Angle

B. Repeatably Experiment

In table I the results of the repeatability experiments are shown. Here, $\mu_{\Delta\alpha_1}$ and $\mu_{\Delta\alpha_2}$ are the average values of the deflection of angle α_1 and α_2 respectively. $\sigma_{\Delta\alpha_1}$ and $\sigma_{\Delta\alpha_2}$ are the standard deviations of the deflection of angle α_1 and α_2 respectively.

TABLE I
REPEATABILITY TEST

Test piece	$\mu_{\Delta\alpha_1}$	$\sigma_{\Delta\alpha_1}$	$\mu_{\Delta\alpha_2}$	$\sigma_{\Delta\alpha_2}$
1	32.9°	2.7°	41.9°	5.8°
2	34.3°	2.3°	43.0°	4.2°
3	30.4°	1.3°	41.6°	2.4°
4	35.1°	2.5°	47.0°	6.4°

C. Implementation into Origami Structure

The implementation of the thermal SMA actuator into the origami inspired gripper resulted in a movement of approximately 10 degrees. This actuation did not result in a gripping movement of the structure.

V. Discussion

The results in figure 8 show a linear relation between the blocking moment and the bending angle. This relationship was expected by equation 3 that follows out of the Brinson model [10]. The SMA NiTiCu wire is able to make a minimum deflection of 30° and repeats the movement five times with a maximum standard deviation of 5°. These

results can be found in table I. All results agree with the set of requirements for the actuator given in section II.

The differences between the three test pieces in figure 8 can be caused by inconsistency during the programming process. The process of manually programming using a blow torch did not have the accuracy needed to make every test piece identical. As a result of not being able to put the same amount of energy in every test piece, the performance of test pieces is different.

While comparing the results of figure 8 with the expected bending moment, difference can be noted between the calculated and measured value. A part of the difference can be explained by the equation 2 used in section III. For this equation an assumptions was made which resulted in the equation 3. When the change of martensite fractions is not neglected, a negative term will be added to the stress as described by the Brinson model which will cause a lower expected generated moment given by equation 2.

Another part to explain the difference, is that during the experiments the thermal SMA wire first have to overcome internal stress in its test piece before it will move to its programmed position. Because of this, the measured blocking moment will be lower than the given moment the SMA wire provides in reality. The blocking moment of the actuator is higher than the generated moment when the SMA wire is not blocked. This means that in the non-blocking situation, the generated moment is lower than shown in figure 8. In figure 2 the estimated stiffness was plotted against the estimated bending moment. The figure 2 shows an intersection of the stiffness and the bending moment at 48.6° when the test piece is configurating towards the straight position. Concluding from the measurements of the experiment, this intersection should be at 77.4°. Whereas looking at the test piece itself, it is found that this angle is approximately 15°. This difference can be explained by the calculation of the hinge moment. For the stiffness of the hinge equation 4 (Howell, 2001) was used which is a linear approach for the hinge that holds in the elastic region [4]. Since the SMA wire deforms plastically, this way to approach the stiffness seems not valid for the hinge.

Last, the NiTiCu wire was not able to actuate the origami-inspired compliant gripper. It seemed that the weight of the structure in combination with the generated moment of the SMA wires resulted in a movement of the gripper. The implemented thermal SMA did not reach a deflection of 30 degrees but approximately 10 degrees. With this deflection of the middle part the finger ends only make a movement of around 5 mm.

VI. Conclusions and recommendations

This research explored the possibility to integrate thermal SMA as an actuator in compliant mechanisms and it was found that this was possible to a certain extent. However, future research should focus on the programming technique of the thermal SMA wire. Ideally, every SMA wire is programmed by putting the same amount of energy in the material at all times. An experiment has proven that thermal SMAs can be programmed by Joule heating, a current of 5 A for 10 minutes is needed. The aluminum mould that has been used during this experiment is conductive, so not suitable for this technique. Another option to program the wire is to make a mould that can be placed in a furnace at 500°C for 30 minutes [12].

Second, further research could focus on the origami design to suit the actuator better. A test showed that the actuation from the middle part was unable to actuate the whole structure. The configuration of the actuation links could have been changed so the wire bends easier. Yet, the design of the origami-inspired compliant mechanism fell outside the scope of this research and, therefore, there was no effort put into it during this study.

Last, a follow up research could focus on the crystalline arrangement and the fraction of martensite within the NiTiCu wire during the actuation. This would enable the researchers to simulate the blocking moments more accurately because the assumption that is made from equation 2 to equation 3 is not needed.

Acknowledgements

This research has been carried out by mechanical engineering bachelor students of Delft University of Technology within the Precision and Microsystems Engineering department. The students are extremely grateful to all supervisors and labsupport within the department for their guidance through the process of this research.

References

[1] An, S.-M., Ryu, J., Cho, M., and Cho, K.-J. Engineering design framework for a shape memory alloy coil spring actuator using a static two-state model. *Smart Materials and Structures 21*, 5 (apr 2012), 055009.

[2] Brinson, L. One-dimensional constitutive behavior of shape memory alloys: Thermomechanical derivation with non-constant material functions and redefined martensite internal variable. *Journal of Intelligent Material Systems and Structures 4*, 2 (1993), 229–242.

[3] Freriks, M. Active origami and kirigami structures - a review of activation methods for distributed transducer systems.

[4] Howell, L. *Compliant Mechanisms*. A Wiley-Interscience publication. Wiley, 2001.

[5] Ikuta, K. Micro/miniature shape memory alloy actuator. In *Proceedings., IEEE International Conference on Robotics and Automation* (May 1990), pp. 2156–2161 vol.3.

[6] Jani, J. M., Leary, M., Subic, A., and Gibson, M. A. A review of shape memory alloy research, applications and opportunities. *Materials Design (1980-2015) 56* (2014), 1078 – 1113.

[7] Konh, B., Datla, N., and Hutapea, P. Feasibility of sma wire actuation for an active steerable cannula. *Journal of Medical Devices 9* (04 2015), 021002–021002.

[8] Magleby, S., C. Greenberg, H., L. Gong, M., and Howell, L. Origami and compliant mechanisms.

[9] Rodrigue, H., Wang, W., Han, M.-W., J.Y. Kim, T., and Ahn, S.-H. An overview of shape memory alloy-coupled actuators and robots. *Soft Robotics 4* (Feb 2017).

[10] Stirbu, B. Constitutive models of shape memory alloys a review.

[11] Tan, W. C., Saad Salleh, A., Jamian, S., and Ghazali, M. I. Phase transformation temperatures for shape memory alloy wire. *Transaction on engineering, computing and technology 19* (01 2007).

[12] Vojtech, D. Influence of heat treatment of shape memory niti alloy on its mechanical properties. *METAL 2010 - 19th International Conference on Metallurgy and Materials, Conference Proceedings* (01 2010), 867–871.